

Article

On the Role of the Cathode for the Electro-Oxidation of Perfluorooctanoic Acid

Alicia L. Garcia-Costa ^{1,2,*} , Andre Savall ² , Juan A. Zazo ¹, Jose A. Casas ¹ and Karine Groenen Serrano ^{2,*}

¹ Chemical Engineering Department, Universidad Autónoma de Madrid, 28049 Madrid, Spain; juan.zazo@uam.es (J.A.Z.); jose.casas@uam.es (J.A.C.)

² Laboratoire de Génie Chimique, Université de Toulouse, CNRS, INPT, UPS, 31062 Toulouse CEDEX 9, France; savall@chimie.ups-tlse.fr

* Correspondence: alicial.garcia@uam.es (A.L.G.C.); serrano@chimie.ups-tlse.fr (K.G.S.)

Received: 22 July 2020; Accepted: 6 August 2020; Published: 8 August 2020



Abstract: Perfluorooctanoic acid (PFOA), $C_7F_{15}COOH$, has been widely employed over the past fifty years, causing an environmental problem because of its dispersion and low biodegradability. Furthermore, the high stability of this molecule, conferred by the high strength of the C-F bond makes it very difficult to remove. In this work, electrochemical techniques are applied for PFOA degradation in order to study the influence of the cathode on defluorination. For this purpose, boron-doped diamond (BDD), Pt, Zr, and stainless steel have been tested as cathodes working with BDD anode at low electrolyte concentration (3.5 mM) to degrade PFOA at 100 mg/L. Among these cathodic materials, Pt improves the defluorination reaction. The electro-degradation of a PFOA molecule starts by a direct exchange of one electron at the anode and then follows a complex mechanism involving reaction with hydroxyl radicals and adsorbed hydrogen on the cathode. It is assumed that Pt acts as an electrocatalyst, enhancing PFOA defluorination by the reduction reaction of perfluorinated carbonyl intermediates on the cathode. The defluorinated intermediates are then more easily oxidized by HO^\bullet radicals. Hence, high mineralization (x_{TOC} : 76.1%) and defluorination degrees (x_{F^-} : 58.6%) were reached with Pt working at current density $j = 7.9 \text{ mA/cm}^2$. This BDD-Pt system reaches a higher efficiency in terms of defluorination for a given electrical charge than previous works reported in literature. Influence of the electrolyte composition and initial pH are also explored.

Keywords: perfluorooctanoic acid; emerging contaminant; defluorination; platinum; electro-oxidation

1. Introduction

Perfluoroalkyl substances (PFAS), such as perfluorooctanoic acid (PFOA, $C_7F_{15}COOH$) are widely used in the chemical industry because of their amphiphilicity, stability, and surfactant property. They are employed in the synthesis of fluoropolymers and fluoroelastomers, as surfactants in fire-fighting foams, and in textile and paper industries to produce water and oil repellent surfaces [1]. Nevertheless, despite their practical interest, these substances present a high toxicity due to their potential bioaccumulation, and common occurrence in water resources. PFOA has been recognized as an emerging environmental pollutant and has been included in the European Candidate List of Substances of Very High Concern (“SVHC”) [2]. Hence, the current challenge is to develop highly efficient and cost-effective processes for the elimination of perfluoroalkyl substances at source.

The main issue in PFOA degradation is to break the C-F bond, one of the strongest bonds known ($\approx 460 \text{ kJ/mol}$) [3]. This confers a high stability and resistance to PFAS which cannot be degraded by direct hydrolysis, photolysis, or through conventional biological treatments [4]. As a result, PFAS

have been detected in natural water streams [5], sediments [6], and even in tap and bottled water in concentrations up to 640 ng/L [7]. So far, adsorption onto carbonaceous materials [8], alumina [9], or other sorbents [10] have been successfully applied for PFAS removal. Nonetheless, this technology implies the transfer of the pollutant to another phase, the sorbent, which becomes a new residue after use. To overcome this drawback, advanced oxidation processes (AOP) are being explored for PFAS removal. AOP are based on the use of strong oxidizing radicals to degrade, most commonly, organic pollutants in aqueous phase [11]. The most extended AOP are those based on the use of hydroxyl radicals (HO^\bullet) to attack organic pollutants by hydrogen abstraction [12]. Consequently, the substitution of all organic hydrogen for fluorine in PFOA makes these compounds inert to this kind of AOP. The non-reactivity of PFOA to HO^\bullet attack has been confirmed by various studies [13–15]. As a matter of fact, Maruthamuthu et al. have shown that the reactivity of hydroxyl radicals on acetate decreases considerably with increasing halogen substitution [13]. Using the Fenton process, known to generate hydroxyl radicals by the action of Fe (II) on hydrogen peroxide, no degradation was observed when the Fenton reagent (0.2 mM, Fe^{2+} : H_2O_2 , molar ratio = 1:1) was mixed with PFOA (0.02 mM) at room temperature [14]. Similar results were obtained by Santos et al. with only 10% PFOA removal and without any C-F bond cleavage [16].

More recently, photocatalytic treatments have been applied for PFOA degradation. This technology achieved high PFOA removal ($x_{\text{PFOA}} > 90\%$) when using modified TiO_2 photocatalysts such as Cu- TiO_2 [17], Pb- TiO_2 [18], and rGO- TiO_2 [19].

Besides PFOA removal, defluorination ($x_{\text{F}^{2212-}}$) is a very important parameter to evaluate the process efficiency. x_{F^-} defined as the ratio of the fluoride concentration ($\text{C}_{\text{F}^-, \text{measured}}$) released by PFOA degradation with respect to the initial content of fluoride in the initial amount of PFOA molecule ($\text{C}_{\text{F}, \text{PFOA } 0}$) is expressed in percentage as shown in Equation (1).

$$x_{\text{F}^-} = \frac{\text{C}_{\text{F}^-, \text{measured}}}{\text{C}_{\text{F}, \text{PFOA } 0}} \cdot 100 \quad (1)$$

In photochemical oxidation of PFOA, defluorination is usually low ($x_{\text{F}^-} < 25\%$), with the average $x_{\text{F}^-}/x_{\text{PFOA}}$ ratio around 0.26 [20].

Another technique for PFAS remediation is electrochemical degradation. PFOA electrooxidation has been successfully carried out in different systems using boron-doped diamond (BDD) as anode (Table 1). Under the studied conditions, PFOA removal ranged from 60% to 100%. It should be noted that defluorination values were very different, suggesting that either the operating conditions (electrolyte, pH, etc.) or the cathode reduction reactions may play a key role in the PFOA degradation mechanism. The cleavage of the C-F bonds to form F^- ions is interesting because F^- ions readily combine with Ca^{2+} to form environmentally harmless CaF_2 , as reported by Hori et al. [3].

x_{F^-} and x_{PFOA} ratios obtained by electrochemical treatment (up to 80–85%, Table 1) are higher than those reported in photo-oxidation (<25%). Nonetheless, all previous electrooxidation studies were conducted employing a high supporting electrolyte concentration, which makes difficult to dispose the treated wastewater after reaction. Therefore, this work aims to gain knowledge on the role of the cathode as electrocatalyst in PFOA electrooxidation working at low electrolyte concentration (3.5 mM). For this purpose, BDD was chosen as the anode and BDD, Pt, Zr, and stainless steel were tested as cathodes in the degradation of 100 mg/L PFOA.

Table 1. Perfluorooctanoic acid (PFOA) electrooxidation with boron-doped diamond (BDD) anode.

Electro-Oxidation System	Operating Conditions	Results	Remarks	Ref
Anode: BDD Cathode: W Area: 38 cm ² Spacing: 4 mm	[PFOA] ₀ : 15 mg/L Electrolyte: 1500 mg/L Na ₂ SO ₄ or 1500 mg/L Na ₂ SO ₄ + 167 mg/L NaCl T: 20 °C, j: 3, 15, 50 mA/cm ² V: 250 mL, t: 480 min	x _{PFOA} : 60–100% x _{F⁻} : 30–80%	No apparent influence of Cl ⁻ in the process	[21]
Anode: BDD Cathode: W Area: 42 cm ² Spacing: 8 mm	[PFOA] ₀ : 100 mg/L Electrolyte: 1.4–8.4 g/L NaClO ₄ , 5 g/L NaSO ₄ T: 20 °C, j: 50, 100, 200 mA/cm ² V: not specified, t: 360 min	x _{PFOA} : 93% x _{TOC} : 95% x _{F⁻} : 38%	In the tested conditions, SO ₄ ²⁻ did not produce additional oxidants. higher j, higher degradation	[22]
Anode: BDD Cathode: BDD Area: 85 cm ² Spacing: 30 mm	[PFOA] ₀ : 50 mg/L Electrolyte: 1.4 g/L NaClO ₄ pH: 3, 9, 12, T: 32 °C, j: 23.24 mA/cm ² V: 40 mL, t: 120 min	x _{PFOA} : 100% x _{F⁻} : 58%	Slightly better results obtained at pH ₀ 3 than pH ₀ 9	[23]
Anode: BDD Cathode: Pt Area: 77.4 cm ² Spacing: 10 mm	[PFOA] ₀ : 50 mg/L Electrolyte: 1.2 g/L NaClO ₄ T: not specified, j: 0.04–1.2 mA/cm ² V: 300 mL, t: 480 min	x _{PFOA} : 85%	F ⁻ deposition on the BDD surface.	[24]
Anode: BDD Cathode: Pt Area: 5.5 cm ² Spacing: 20 mm	[PFOA] ₀ : 200 mg/L Electrolyte: 7.1 g/L Na ₂ SO ₄ P: 0.3 MPa, T: 80–120 °C, j: 20 mA/cm ² V: 400 mL, t: 360 min	x _{PFOA} : 95% x _{TOC} : 90% x _{F⁻} : 90%	High temperature process greatly enhances the PFOA degradation in relation to the room temperature system.	[25]

2. Results and Discussion

In order to test the influence of the cathode material on the degradation process, a BDD anode was successively coupled with cathodes made of BDD, Pt, Zr, and stainless steel. Results of electrolysis runs conducted at 7.9 mA/cm², at 25 °C, for the treatment of 100 mg/L PFOA solutions (namely, 0.242 mol/m³), are presented in Figure 1a. For each couple of electrodes, the curves show that PFOA concentration followed, from C_{PFOA,0} = 100 mg/L to C_{PFOA,t} ≈ 25 mg/L, a similar decrease, characteristic of a pseudo-first order kinetics. For experiments presented in Figure 1a the applied current density was higher than the limiting current density. Considering a pure mass transport controlled reaction for the first exchange of charge between a molecule of PFOA and the anode surface, the limiting current density calculated using the equation established from the Nernst diffusion model: $j_{lim} = n \cdot F \cdot k_m \cdot C_{PFOA,0}$ equals to 0.63 A/m² for $n = 1$, $F = 96,485$ C/mol, $k_m = 2.7 \cdot 10^{-5}$ m/s (determined experimentally using the ferri/ferro system, as described elsewhere [26]) for a flow rate of 0.360 m³/h [27], C_{PFOA,0} = 0.242 mol/m³. This value of the limiting current density is more than 100 times lower than that applied during electrolysis ($j = 79$ A/m²). Under these conditions, the decay of concentration from C_{PFOA,0} to C_{PFOA,t} depends upon the mass transfer coefficient k_m , the surface area (A) of the electrode, and the volume (V) of electrolyte [28], as follows:

$$C_{PFOA,t} = C_{PFOA,0} \cdot e^{\left(\frac{-1}{\tau}\right)} \quad (2)$$

where the constant of time, τ , is defined by: $\tau = V/(k_m A)$. For its calculation we considered the following values $V = 10^{-3}$ m³, $A = 63 \cdot 10^{-4}$ m², and $k_m = 2.7 \cdot 10^{-5}$ m/s, obtaining a time constant (τ) equal to 5800 s. According to Equation (2), the PFOA theoretical concentration at $t = 2$ h is around 29 mg/L, which is in agreement with the experimental results (≈25 mg/L), as shown in Figure 1a.

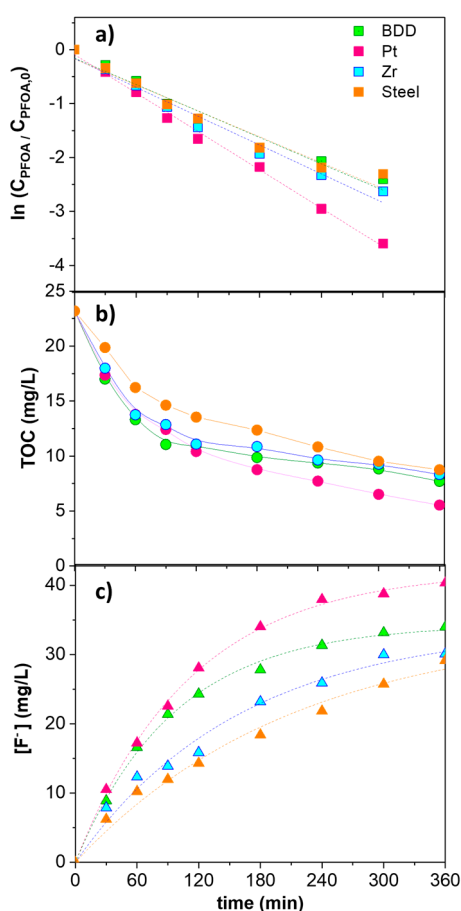


Figure 1. Influence of the cathode material in (a) PFOA removal (symbols: experimental data, lines: kinetic fitting), (b) TOC depletion, (c) released fluoride (symbols: experimental data, lines: kinetic fitting). Operating conditions: $[PFOA]_0$: 100 mg/L, j : 7.9 mA/cm², electrolyte: 3.5 mM Na₂SO₄, T: 25 °C, pH₀: 4.

The excess of charge on the first oxidation step of PFOA is used for other electron transfers and by the action of HO• radicals during the degradation of the numerous intermediates. PFOA removal after 6 h was 100%, 98.1%, 97.9%, and 97.6% for Pt, steel, Zr, and BDD, respectively. Values of the rate constants and regression coefficients are collected in Table 2. It should be noted that the Pt cathode has the best results with a PFOA degradation rate 39% faster than the other tested materials, which exhibit a similar behavior between them. This enhancement is also reflected in the mineralization degree (Figure 1b), with a 76.1% Total Organic Carbon (TOC) removal with the BDD-Pt system.

Table 2. PFOA degradation and fluoride release kinetics.

	$k_{PFOA} \cdot 10^3 \text{ (min}^{-1}\text{)}$	r^2	$k_{F^-} \cdot 10^3 \text{ (min}^{-1}\text{)}$	r^2
BDD	8.92 ± 0.68	0.988	8.97 ± 0.28	0.999
Pt	11.86 ± 0.32	0.994	10.36 ± 0.44	0.997
Zr	8.16 ± 0.58	0.979	6.23 ± 0.86	0.982
Steel	7.98 ± 0.42	0.981	4.70 ± 0.78	0.982

As previously explained, one of the main challenges in PFOA oxidation is the effective breakdown of the C-F bond. PFOA defluorination was followed along the reaction by means of ionic chromatography, as depicted in Figure 1c. The trend for defluorination was Pt > BDD > Zr > steel. In this case, the cathode also played an important role, reaching a 58.6% in the case of Pt, against 42–49% for BDD,

Zr, and steel. Moreover, fluoride release follows a first order, as reflected in Figure 1 and Table 2, where the function of Pt as electrocatalyst is confirmed.

Pt is a common catalyst in hydrodehalogenation reaction of organic molecules, because of its capacity to adsorb hydrogen, providing a catalytic site where the dehalogenation takes place [29]. H_2 generation by water electrolysis on the cathode's surface may be responsible for PFOA hydrodefluorination, following the reaction mechanism shown in Figure 2.

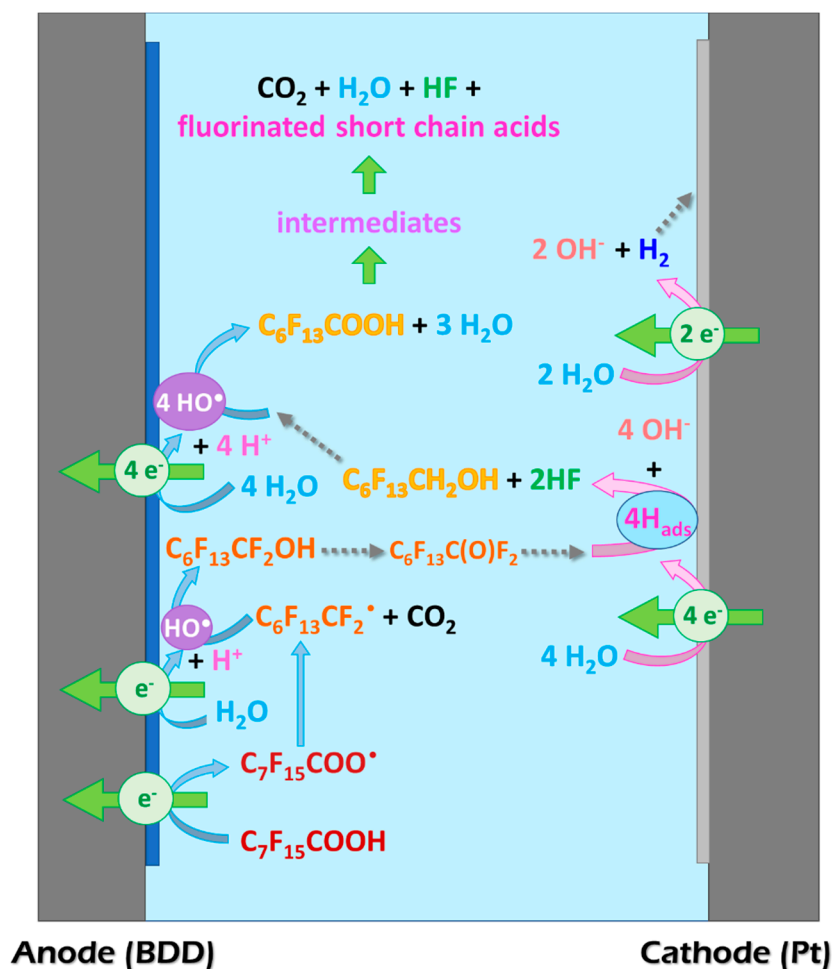
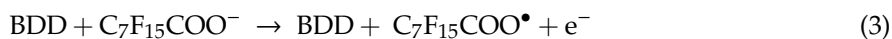


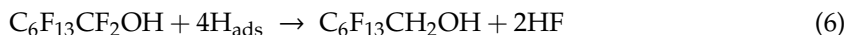
Figure 2. PFOA electrooxidation mechanism.

Because PFOA is inert to hydroxyl radicals, its degradation is initiated on the anode by a direct electron transfer reaction to form a perfluoro radical C₇F₁₅COO• (Equation (3)). This radical loses its carboxylic group (Equation (4)) and reacts with HO• leading to the generation of C₆F₁₃CF₂OH (Equation (5)), as previously described by Zhang et al. [30].



This alcohol then reacts according to three pathways, (for clarity reasons, only the first one (i) is illustrated in Figure 2):

- (i) With adsorbed hydrogen generated by water electro-reduction at the cathode, releasing 2 F[−] (Equation (6)).



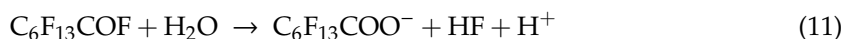
As the first carbon in the alkyl chain is now defluorinated, HO• can attack it once again leading to the formation of C₆F₁₃COOH. This mechanism is similar to that presented for PFOA photocatalytic degradation by Wang et al. [20] and theoretic quantum calculations and experimental data collected by Trojanowicz et al. [31]. Hence, this step depends strongly on the cathode material.

- (ii) With hydroxyl radicals leading to the formation of COF₂, as related by Niu et al. [31] and Zhang et al. [28], following Equations (7)–(9):



According to George et al. [30] hydrolysis of carbonyl fluoride COF₂ in the aqueous phase is extremely fast since its half-life is 0.7 s at T = 273 K.

- (iii) Giving the perfluorocarbonyl fluoride (Equation (10)) for which hydrolysis leads the formation of perfluorocarboxylic acid and HF (Equation (11)) [30,32].



Considering this complex reaction mechanism, it should be noted that TOC decay was faster within the first hour of reaction, then it slowed down (Figure 1b). This is related to the generation of short-chain fluorinated acids (decarboxylation step), which are less active to electro-oxidation processes. In fact, pH value in the Pt system decreased from 4 to 3.2 in 120 min, maintaining this pH until the end of the reaction, which evidences the generation of these acidic species.

Data displayed in Figure 1 allow to determine the fluoride concentrations produced with respect to the degraded carbon in the form of CO₂ (F[−]/CO₂) or with respect to the PFOA eliminated over time (F[−]/PFOA). Figure 3 shows that the PFOA defluorination leads to the formation of 1 to 1.5 fluorine ions per removed atom of carbon in the first three hours of electrolysis. According to the proposed mechanism, this value close to the one at the beginning of the electrolysis is related to decarboxylation which leads to the formation of R_f-COF. The kinetics of this step are probably faster than that of the defluorination stages according to Equations (6)–(9). Besides, part of the process can be attributable to the electrocatalytic hydrogenation of the perfluorocarbonyl fluoride C₆F₁₃COF that forms simultaneously the hydrofluoric acid and the 1,1-dihydroperfluoroalkyl alcohol C₆F₁₃CH₂OH. This alcohol is stable but easily oxidizable on the BDD anode [33] (cf. Figure 2). This process is slowed down by the diffusion of the species to the cathode. Not all molecules undergo the loss of two fluoride atoms, which would explain the value of 1.5 instead of the usual ratio 1.9 present in the initial PFOA molecule.

In addition, Figure 3 shows the variation of the ratio between the concentration of fluoride ions released and the concentration of the removed PFOA. This ratio varies from 7.7 to 9 for 360 min of electrolysis. These values highlight the high, yet incomplete PFOA defluorination. Finally, the ratio between the carbon loss (in the form of CO₂) and the removed PFOA (CO₂/PFOA) is in the order of 6–7, slightly less than 8, i.e., the theoretical value for C₇F₁₅COOH, confirming the formation of reaction intermediates. This ratio decreases during electrolysis: the degradation being faster at the beginning of the reaction, until t:150 min.

At this time more than 85% of PFOA has been eliminated. PFOA depletion slows down both the defluorination and carbon skeleton breaking. In addition, shorter molecular chains could display slower kinetics.

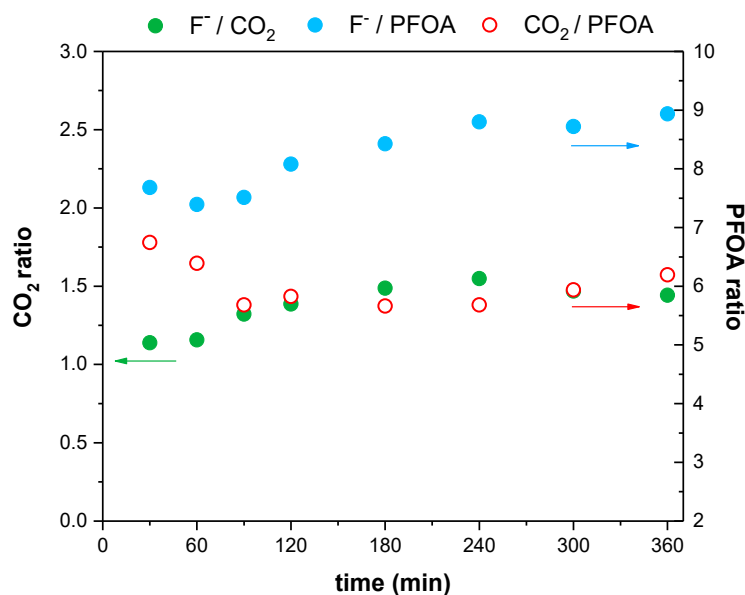


Figure 3. Variation of fluorine ions (full symbols) and carbon removal (empty symbols) during electrolysis with respect to carbon removal and degraded PFOA. Operating conditions: $[PFOA]_0$: 100 mg/L, j : 7.9 mA/cm², electrolyte: 3.5 mM Na₂SO₄, T: 25 °C, pH₀: 4.

Figure 4 shows the ratio of fluorine and carbon atoms contained in the chemical intermediates. The molar concentration of F and C atoms contained in the intermediates are defined, respectively, as follows:

$$C_{F,intermediates} = 15 \cdot (C_{PFOA,0} - C_{PFOA,t}) - C_{F-t} \quad (12)$$

$$C_{C,intermediates} = TOC_t - TOC_{PFOA,t} \quad (13)$$

where $C_{PFOA,0}$ and $C_{PFOA,t}$ refer to the molar concentration of PFOA at initial time and at time t , respectively; C_{F-t} is the molar concentration of fluorine ions at t ; TOC_t and $TOC_{PFOA,t}$ are the total carbon molar concentration and the carbon molar concentration in the PFOA, respectively.

From Figure 1, after 360 min of electrolysis, the defluorination rate is 59% whereas more than 98% of PFOA and 76% of TOC have been eliminated. Figure 4 highlights that in this moment, the intermediates still contain 24% of carbon and 41% of fluorine. Xiao et al. reached a 90% defluorination and mineralization working at high temperature (T: 80–120 °C), meaning they managed to degrade the short-chain acids [25]. This is in agreement with the results for degradation of phenol in heterogeneous Fenton at high temperature, where maleic, malonic, oxalic, and formic acids can be completely degraded [11], in contrast with room temperature processes [34]. Aiming to verify Xiao et al.'s results, an electrooxidation run at 80 °C was performed using Pt cathode. After 30 min reaction there was an overvoltage on the cell due to the damage on the cathode, probably because of the HF attack (Figure S1 of the Supplementary Material). Hence, high temperature electrooxidation could not be performed in our system and further runs were conducted at 25 °C.

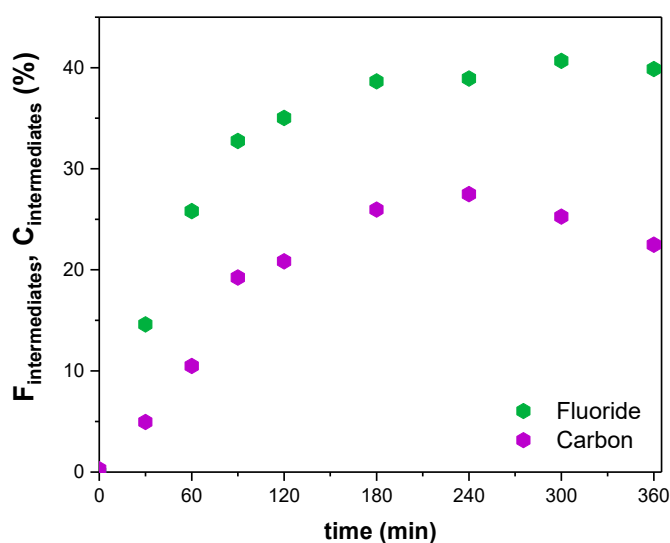
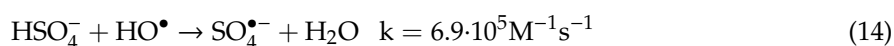


Figure 4. Ratio of fluorine and carbon atoms in the chemical intermediates. Operating conditions: [PFOA]₀: 100 mg/L, *j*: 7.9 mA/cm², electrolyte: 3.5 mM Na₂SO₄, T: 25 °C, pH₀: 4.

After selecting Pt as the best cathode, within the tested materials, different salts were used as electrolyte, NaClO₄, KNO₃, Na₂SO₄, Na₂S₂O₈, at 3.5 mM. Results for these experiments can be found in Figure 5. As previously reported by Schaefer et al. [21], the influence of the electrolyte type on PFOA degradation is very low. Still, significant differences were found for TOC removal, where the removal efficiency followed this trend Na₂SO₄ (76.1%) > Na₂S₂O₈ (72.6%) > KNO₃ (70.5%) > NaClO₄ (67.1%). Sulfate achieved both a slightly higher mineralization degree and defluorination. This can be explained by the fact that sulfate anions behave as an active electrolyte via the electrochemical generation of the strong oxidizing sulfate radicals (SO₄^{•−}) on a BDD anode [35,36]. Indeed, the oxidation of water at the anode greatly decreases locally the pH at the surface leading to the formation of HSO₄[−] from SO₄^{2−}. Then HSO₄[−] reacts with HO[•] radicals to form sulfate radicals [33,37].



SO₄^{•−} radical participates in electron transfer reactions and promotes the decarboxylation of carboxylic acids, contrary to HO[•] which rather acts in hydrogen abstraction or addition [38]. In addition, sulfate radicals are more stable than hydroxyl radicals (their half-life is 30–40 μs and 10^{−3} μs, respectively).

Considering PFOA degradation with sulfate radicals, the literature review by Yang et al. highlights that the decomposition and defluorination efficiencies increase with a decrease in PFOA chain-length [39]. Besides the major role of hydroxyl radicals on PFOA oxidation, the presence of sulfate radicals helps to improve the degradation of the generated intermediates. Qian et al. [40] estimated the constant rate of PFOA degradation with sulfate radicals at 2.59 · 10⁵ M^{−1} s^{−1}. This is consistent with the higher TOC removal observed in our experiments in presence of sulfate. Furthermore, sulfate is a more environmentally friendly electrolyte, in comparison to perchlorate and nitrate, which can be considered pollutants by themselves. Thus, the rest of experiments were carried out using Na₂SO₄ 3.5 mM.

Influence of initial pH (pH₀) on PFOA degradation was also evaluated working at the natural pH of PFOA solution (pH: 4) and at pH values of 7 and 9. Results for these experiments are shown in Figure 6. As it may be seen in Figure 6d, reaction media is quickly acidified. This is related to both the generation of short chain acids and the reaction between sulfate radicals and water to produce hydroxyl radicals, which also generates protons, as depicted in Equation (15). PFOA decay (Figure 6a) was similar for all the runs. However, pH₀ had a great influence on the initial rate for TOC abatement,

related to the higher oxidation potential of sulfate radicals in alkaline media [41]. Despite achieving a higher mineralization degree at pH_0 : 9, the highest defluorination was reached when starting in acidic media.

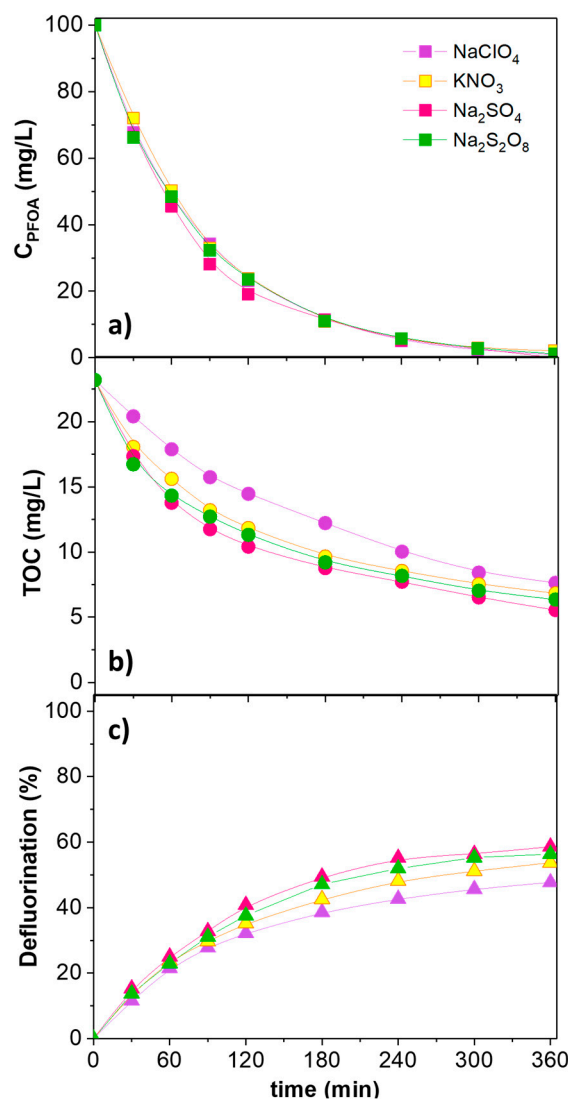
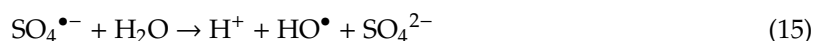


Figure 5. Influence of the electrolyte in PFOA (a) degradation, (b) mineralization, and (c) defluorination in electrooxidation using BDD/Pt electrodes. Operating conditions: $[\text{PFOA}]_0$: 100 mg/L, j : 7.9 mA/cm², electrolyte: 3.5 mM, T : 25 °C, pH_0 : 4.

So far, the role of the cathode as electrocatalyst in the degradation and defluorination of PFOA has been proved. Also, the influence of several operating conditions has been tested, demonstrating an overall great decontamination working at low electrolyte concentration at mild temperature. Nonetheless, in order to compare the obtained results with those reported in literature, we have compared the defluorination degree against the energetic requirements, measured as the applied charge, as shown in Figure 7. As may be seen, both Shaefer et al. [21] and Urtiaga et al. [22] boosted the defluorination degree when increasing the applied charge. However, the results presented in this work using Pt cathode at 7.9 mA/cm², 3.5 mM Na₂SO₄ at pH_0 :4 and T :25 °C are the most competitive in terms of PFOA defluorination against electric charge. In this sense, cathode selection becomes a key point for both increasing the activity and reducing the energy requirements in PFOA electrooxidation.

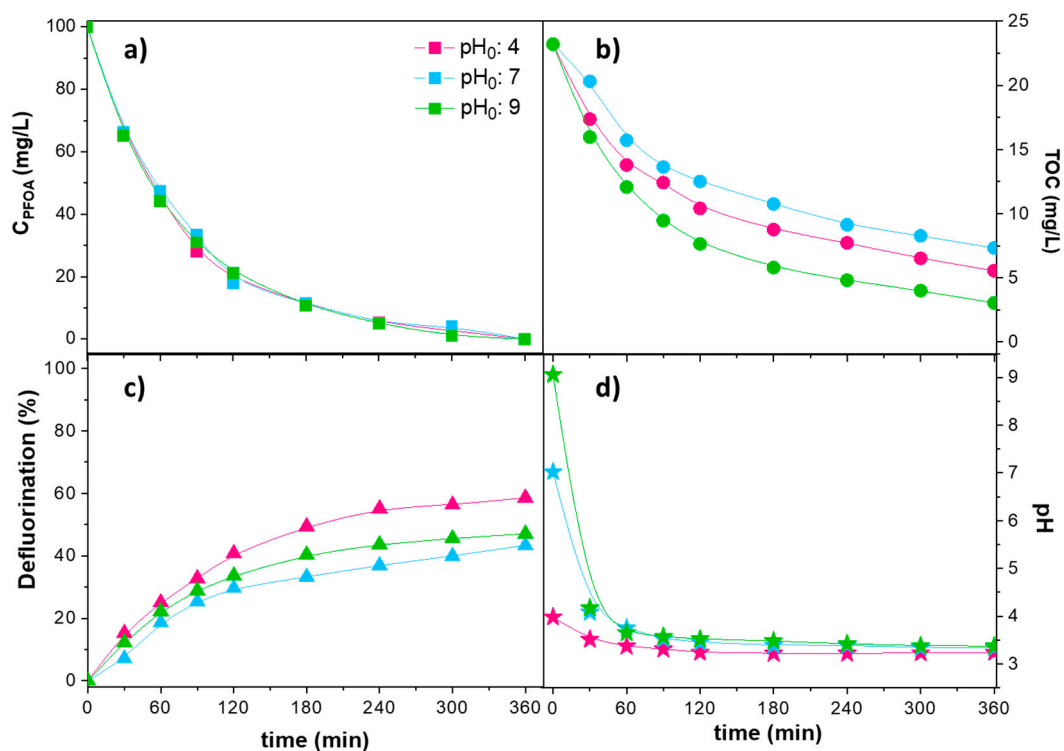


Figure 6. Influence of the pH_0 in PFOA (a) degradation, (b) mineralization, and (c) defluorination and (d) pH evolution in electrooxidation using BDD/Pt electrodes. Operating conditions: $[PFOA]_0$: 100 mg/L, j : 7.9 mA/cm², Na_2SO_4 : 3.5 mM, T : 25 °C.

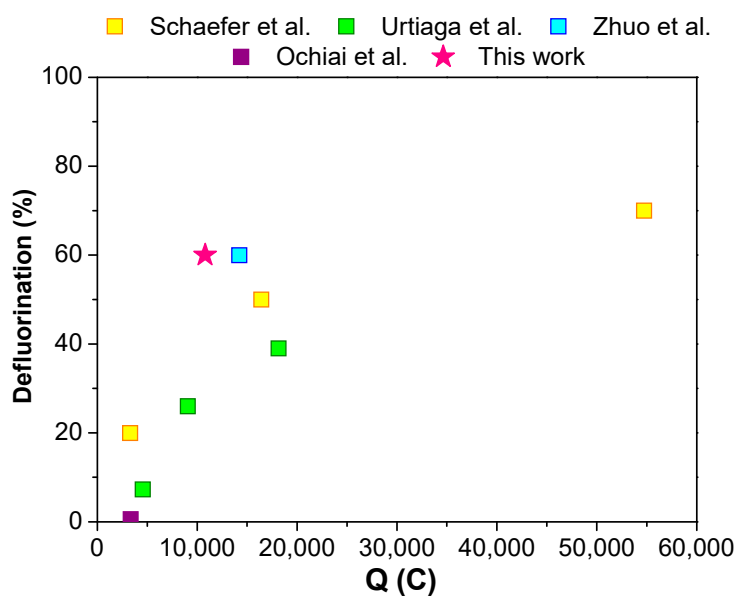


Figure 7. Process comparison in terms of defluorination against electric charge for PFOA electrooxidation with BDD anodes. Cathodes: Schaefer et al.—W [21], Urtiaga et al.—W [22], Zhuo et al.—BDD [23], Ochiai et al.—Pt [24], this work—Pt.

3. Materials and Methods

3.1. Reactants

Perfluorooctanoic acid (95 wt.%), Na_2SO_4 , KNO_3 , NaClO_4 , $\text{Na}_2\text{S}_2\text{O}_8$, acetonitrile (ACN), H_2SO_4 , and NaOH were supplied by Sigma-Aldrich (Darmstadt, Germany). All reagents are of analytical grade and they were used as received without further purification. Working standard solutions of PFOA and fluoride (NaF from Sigma-Aldrich, Darmstadt, Germany) were prepared for calibration.

3.2. Experimental Set-Up

The electrochemical oxidation system consists in a 1-L thermoregulated glass reservoir connected to the cell through a centrifugal pump. PFOA solution was recycled in the system at 360 L/h flow rate and the temperature was set at 25 ± 1 °C. The electrochemical cell is a one-compartment flow filter-press reactor which was operated under galvanostatic conditions using an ELCAL 924 power supply (Italy). Electrodes present a 63 cm^2 active surface and the gap between them was set at 10 mm. A detailed scheme of the experimental set-up can be found elsewhere [42]. All experiences were performed with a BDD anode from Adamant Technologies (La Chaux-de-Fonds, Switzerland), which was elaborated by chemical vapor deposition on a conductive substrate of Si. BDD (Adamant Technologies, La Chaux-de-Fonds, Switzerland), Zirconium, Stainless steel, and Pt (5 μm) on titanium substrate (provided by MAGNETO special anodes B.V., Schiedam, Netherlands) were employed as cathodes. Before each electrolysis, the working electrodes were anodically pretreated (40 mA/cm^2 for 30 min in 0.1 M H_2SO_4) to clean their surfaces of any possible adsorbed impurities. Then, the system was rinsed by ultrapure water.

In a typical reaction 1 L PFOA solution (100 mg/L) with 3.5 mM Na_2SO_4 as electrolyte at the natural pH of the solution (pH:4) was loaded to the reservoir, preheated to 25 °C and recycled through the system. Once the selected temperature was reached, the power supply was turned on and current intensity was set at 0.5 A, representing this as the reaction starting time. Samples were taken at regular intervals in the tank. The global volume of samples was less than 10% of the total volume. All runs were performed by triplicate with a deviation lower than 5% in all cases.

3.3. Analytical Methods

Samples were periodically withdrawn from the reactors, filtered through 0.2 μm nylon syringe plug-in filters and immediately analyzed, without any further manipulation. PFOA concentration was measured by high performance liquid chromatography connected with an ultraviolet-visible spectrometry detector (HPLC-UV Agilent 1200 Series HPLC, Santa Clara, USA). An ion-exclusion column (ZORBAX Eclipse Plus C18, 100 mm, 1.8 μm , Agilent, USA) was used as the stationary phase. As mobile phase mixture of ACN/4 mM H_2SO_4 aqueous solution with a ratio: 3/2 was employed and the column temperature was set to 50 °C. A 60% CAN—40% mixture was employed at 0.5 mL/min. The detection UV wavelength was set to 206 nm. Total organic carbon was quantified using a TOC analyzer (Shimadzu TOC-VSCH, Kyoto, Japan). Fluoride was analyzed in an ion chromatograph with chemical suppression (Metrohm 790 IC, Herisau, Switzerland) using a conductivity detector. A Metrosep A supp 5–250 column (25 cm long, 4 mm diameter, Herisau, Switzerland) was used as the stationary phase and 0.7 mL/min of a 3.2 mM/1 mM aqueous solution of Na_2CO_3 and NaHCO_3 , respectively, as the mobile phase.

4. Conclusions

PFOA electro-degradation follows a complex mechanism which involves both oxidation reactions on the anode surface and reduction reactions, responsible for the molecule's defluorination, which take place over the cathode. Electrocatalytic hydrogenation of the unsaturated acyl fluoride R_fCOF can be a route for the degradation process. Atomic hydrogen produced in situ at the catalyst surface can form simultaneously the alcohol RFCH_2OH and hydrofluoric acid.

In this work, different cathodes have been used, finding that its selection plays a key role in PFOA degradation. In this sense, Pt acts as an electrocatalyst because of its higher capacity to produce in situ atomic hydrogen, which seems efficient in hydrodefluorination. It has been also demonstrated that working at low electrolyte concentration (3.5 mM Na₂SO₄), complete PFOA removal can be reached with up to 76.1% TOC abatement and 58.6% defluorination working at the natural pH of the solution (pH₀: 4). The kind of electrolyte employed did not have a significant impact on the overall reaction. Still, slightly better results were achieved using sulfate because of the generation of sulfate radicals. Regarding the influence of the starting pH, higher TOC removal was obtained working at pH₀: 9, while at higher pH values PFOA mineralization was hindered. When comparing the results obtained in this work with those reported in literature, it must be remarked that the employed BDD-Pt system allows a higher defluorination degree with a lower energy consumption. In view to render the process economically viable to treat dilute solutions, further experiments are planned to combine the electrochemical process with a preconcentration step (such as filtration or adsorption).

Supplementary Materials: The following are available online at <http://www.mdpi.com/2073-4344/10/8/902/s1>, Figure S1. Damaged Pt cathode after high temperature PFOA electrooxidation (T: 80 °C).

Author Contributions: A.L.G.C.: conceptualization, investigation, data curation, methodology, writing: original draft. J.A.Z.: supervision, writing: review. A.S.: supervision, data curation, validation, writing: review. K.G.S.: formal analysis, supervision, validation, writing: review. J.A.C.: formal analysis, funding acquisition, supervision, validation, writing: review. All authors have read and agreed to the published version of the manuscript.

Funding: This research was funded by the Spanish Ministerio de Ciencia, Innovación y Universidades through project CTM2016-76454-R and by Comunidad de Madrid by P2018/EMT-4341 REMTAVARES-CM.

Acknowledgments: Authors thank the funding received from Ministerio de Ciencia, Innovación y Universidades through research project CTM2016-76454-R and Comunidad de Madrid for P2018/EMT-4341 REMTAVARES-CM. Alicia L. Garcia-Costa would like to thank Campus France for the mobility grant under the Make Our Planet Great Again (MOPGA) program and the Spanish Ministerio de Ciencia, Innovación y Universidades for mobility grant EST2019-013106-I. She would also like to thank both the Spanish Ministerio de Economía y Competitividad and the European Social Fund for the PhD grant BES-2014-067598.

Conflicts of Interest: The authors declare no conflict of interest.

References

1. Gebbink, W.A.; van Leeuwen, S.P.J. Environmental Contamination and Human Exposure to PFASs Near a Fluorochemical Production Plant: Review of Historic and Current PFOA and GenX Contamination in the Netherlands. *Environ. Int.* **2020**, *137*, 11. [[CrossRef](#)] [[PubMed](#)]
2. Ao, J.J.; Yuan, T.; Xia, H.; Ma, Y.N.; Shen, Z.M.; Shi, R.; Tian, Y.; Zhang, J.; Ding, W.J.; Gao, L.; et al. Characteristic and Human Exposure Risk Assessment of Per- and Polyfluoroalkyl Substances: A study Based on Indoor Dust and Drinking Water in China. *Environ. Pollut.* **2019**, *254*, 9. [[CrossRef](#)] [[PubMed](#)]
3. Hori, H.; Hayakawa, E.; Einaga, H.; Kutsuna, S.; Koike, K.; Ibusuki, T.; Kiatagawa, H.; Arakawa, R. Decomposition of Environmentally Persistent Perfluorooctanoic Acid in Water by Photochemical Approaches. *Environ. Sci. Technol.* **2004**, *38*, 6118–6124. [[CrossRef](#)] [[PubMed](#)]
4. Kannan, K.; Koistinen, J.; Beckmen, K.; Evans, T.; Gorzelany, J.F.; Hansen, K.J.; Jones, P.D.; Helle, E.; Nyman, M.; Giesy, J.P. Accumulation of Perfluorooctane Sulfonate in Marine Mammals. *Environ. Sci. Technol.* **2001**, *35*, 1593–1598. [[CrossRef](#)]
5. Wang, G.H.; Wang, X.L.; Xing, Z.N.; Lu, J.J.; Chang, Q.G.; Tong, Y.B. Occurrence and Distribution of Perfluorooctane Sulfonate and Perfluorooctanoic Acid in Three Major Rivers of Xinjiang, China. *Environ. Sci. Pollut. Res.* **2019**, *26*, 28062–28070. [[CrossRef](#)]
6. Pico, Y.; Blasco, C.; Farre, M.; Barcelo, D. Occurrence of Perfluorinated Compounds in Water and Sediment of L'Albufera Natural Park (Valencia, Spain). *Environ. Sci. Pollut. Res.* **2012**, *19*, 946–957. [[CrossRef](#)]
7. Domingo, J.L.; Nadal, M. Human Exposure to Per-And Polyfluoroalkyl Substances (PFAS) through Drinking Water: A Review of the Recent Scientific Literature. *Environ. Res.* **2019**, *177*, 10. [[CrossRef](#)]
8. Saeidi, N.; Kopinke, F.D.; Georgi, A. Understanding the Effect of Carbon Surface Chemistry on Adsorption of Perfluorinated Alkyl Substances. *Chem. Eng. J.* **2020**, *381*, 11. [[CrossRef](#)]

9. Wang, F.; Shih, K.M. Adsorption of Perfluorooctanesulfonate (PFOS) and Perfluorooctanoate (PFOA) on Alumina: Influence of Solution pH and Cations. *Water Res.* **2011**, *45*, 2925–2930.
10. Maimaiti, A.; Deng, S.B.; Meng, P.P.; Wang, W.; Wang, B.; Huang, J.; Wang, Y.J.; Yu, G. Competitive Adsorption of Perfluoroalkyl Substances on Anion Exchange Resins in Simulated AFFF-Impacted Groundwater. *Chem. Eng. J.* **2018**, *348*, 494–502. [[CrossRef](#)]
11. Garcia-Costa, A.L.; Zazo, J.A.; Casas, J.A. Microwave-Assisted Catalytic Wet Peroxide Oxidation: Energy Optimization. *Sep. Purif. Technol.* **2019**, *215*, 62–69. [[CrossRef](#)]
12. Garcia-Costa, A.L.; Zazo, J.A.; Rodriguez, J.J.; Casas, J.A. Intensification of Catalytic Wet Peroxide Oxidation With Microwave Radiation: Activity and Stability of Carbon Materials. *Sep. Purif. Technol.* **2019**, *209*, 301–306. [[CrossRef](#)]
13. Maruthamuthu, P.; Padmaja, S.; Huie, R.E. Rate Constants for Some Reactions of Free-Radicals with Haloacetates in Aqueous-Solution. *Int. J. Chem. Kinet.* **1995**, *27*, 605–612. [[CrossRef](#)]
14. Moriwaki, H.; Takagi, Y.; Tanaka, M.; Tsuruho, K.; Okitsu, K.; Maeda, Y. Sonochemical Decomposition of Perfluorooctane Sulfonate and Perfluorooctanoic Acid. *Environ. Sci. Technol.* **2005**, *39*, 3388–3392. [[CrossRef](#)] [[PubMed](#)]
15. Javed, H.; Lyu, C.; Sun, R.N.; Zhang, D.N.; Alvarez, P.J.J. Discerning the Inefficacy of Hydroxyl Radicals during Perfluorooctanoic Acid Degradation. *Chemosphere* **2020**, *247*, 6. [[CrossRef](#)]
16. Santos, A.; Rodriguez, S.; Pardo, F.; Romero, A. Use of Fenton Reagent Combined with Humic Acids for the Removal of PFOA from Contaminated Water. *Sci. Total Environ.* **2016**, *563*, 657–663. [[CrossRef](#)]
17. Chen, M.J.; Lo, S.L.; Lee, Y.C.; Huang, C.C. Photocatalytic Decomposition of Perfluorooctanoic Acid by Transition-Metal Modified Titanium Dioxide. *J. Hazard. Mater.* **2015**, *288*, 168–175. [[CrossRef](#)]
18. Chen, M.J.; Lo, S.L.; Lee, Y.C.; Kuo, J.; Wu, C.H. Decomposition of Perfluorooctanoic Acid by Ultraviolet Light Irradiation with Pb-Modified Titanium Dioxide. *J. Hazard. Mater.* **2016**, *303*, 111–118. [[CrossRef](#)]
19. Gomez-Ruiz, B.; Ribao, P.; Diban, N.; Rivero, M.J.; Ortiz, I.; Urtiaga, A. Photocatalytic Degradation and Mineralization of Perfluorooctanoic Acid (PFOA) Using a Composite TiO₂-rGO Catalyst. *J. Hazard. Mater.* **2018**, *344*, 950–957. [[CrossRef](#)]
20. Wang, S.N.; Yang, Q.; Chen, F.; Sun, J.; Luo, K.; Yao, F.B.; Wang, X.L.; Wang, D.B.; Li, X.M.; Zeng, G.M. Photocatalytic Degradation of Perfluorooctanoic Acid and Perfluorooctane Sulfonate in Water: A Critical Review. *Chem. Eng. J.* **2017**, *328*, 927–942. [[CrossRef](#)]
21. Schaefer, C.E.; Andaya, C.; Burant, A.; Condee, C.W.; Urtiaga, A.; Strathmann, T.J.; Higgins, C.P. Electrochemical Treatment of Perfluorooctanoic Acid and Perfluorooctane Sulfonate: Insights into Mechanisms and Application to Groundwater Treatment. *Chem. Eng. J.* **2017**, *317*, 424–432. [[CrossRef](#)]
22. Urtiaga, A.; Fernandez-Gonzalez, C.; Gomez-Lavin, S.; Ortiz, I. Kinetics of the Electrochemical Mineralization of Perfluorooctanoic Acid on Ultrananocrystalline Boron Doped Conductive Diamond Electrodes. *Chemosphere* **2015**, *129*, 20–26. [[CrossRef](#)] [[PubMed](#)]
23. Zhuo, Q.F.; Deng, S.B.; Yang, B.; Huang, J.; Wang, B.; Zhang, T.T.; Yu, G. Degradation of Perfluorinated Compounds on a Boron-Doped Diamond Electrode. *Electrochim. Acta* **2012**, *77*, 17–22. [[CrossRef](#)]
24. Ochiai, T.; Iizuka, Y.; Nakata, K.; Murakami, T.; Tryk, D.A.; Fujishima, A.; Koide, Y.; Morito, Y. Efficient Electrochemical Decomposition of Perfluorocarboxylic Acids by the Use of a Boron-Doped Diamond Electrode. *Diam. Relat. Mater.* **2011**, *20*, 64–67. [[CrossRef](#)]
25. Xiao, H.S.; Lv, B.Y.; Zhao, G.H.; Wang, Y.J.; Li, M.F.; Li, D.M. Hydrothermally Enhanced Electrochemical Oxidation of High Concentration Refractory Perfluorooctanoic Acid. *J. Phys. Chem. A* **2011**, *115*, 13836–13841. [[CrossRef](#)]
26. Mais, L.; Mascia, M.; Palmas, S.; Vacca, A. Photoelectrochemical Oxidation of Phenol With Nanostructured TiO₂-PANI Electrodes under Solar Light Irradiation. *Sep. Purif. Technol.* **2019**, *208*, 153–159. [[CrossRef](#)]
27. Weiss, E.; Groenen-Serrano, K.; Savall, A.; Comninellis, C. A Kinetic Study of the Electrochemical Oxidation of Maleic Acid on Boron Doped Diamond. *J. Appl. Electrochem.* **2007**, *37*, 41–47. [[CrossRef](#)]
28. Walsh, F.C. A First Course in Electrochemical Engineering. *The Electrochemical Consultancy.* **1993**, 381. [[CrossRef](#)]
29. Pizarro, A.H.; Molina, C.B.; Fierro, J.L.G.; Rodriguez, J.J. On the Effect of Ce Incorporation on Pillared Clay-Supported Pt and Ir Catalysts for Aqueous-Phase Hydrodechlorination. *Appl. Catal. B Environ.* **2016**, *197*, 236–243. [[CrossRef](#)]

30. Zhang, Y.Y.; Moores, A.; Liu, J.X.; Ghoshal, S. New Insights into the Degradation Mechanism of Perfluorooctanoic Acid by Persulfate from Density Functional Theory and Experimental Data. *Environ. Sci. Technol.* **2019**, *53*, 8672–8681. [[CrossRef](#)]
31. Trojanowicz, M.; Bojanowska-Czajka, A.; Bartosiewicz, I.; Kulisa, K. Advanced Oxidation/Reduction Processes Treatment for Aqueous Perfluorooctanoate (PFOA) and Perfluorooctanesulfonate (PFOS)—A Review of Recent Advances. *Chem. Eng. J.* **2018**, *336*, 170–199. [[CrossRef](#)]
32. Niu, J.F.; Lin, H.; Gong, C.; Sun, X.M. Theoretical and Experimental Insights into the Electrochemical Mineralization Mechanism of Perfluorooctanoic Acid. *Environ. Sci. Technol.* **2013**, *47*, 14341–14349. [[CrossRef](#)] [[PubMed](#)]
33. Stefanova, A.; Ayata, S.; Erem, A.; Ernst, S.; Baltruschat, H. Mechanistic Studies on Boron-Doped Diamond: Oxidation of Small Organic Molecules. *Electrochim. Acta* **2013**, *110*, 560–569. [[CrossRef](#)]
34. Zazo, J.A.; Casas, J.A.; Mohedano, A.F.; Rodriguez, J.J. Catalytic Wet Peroxide Oxidation of Phenol with a Fe/active Carbon Catalyst. *Appl. Catal. B Environ.* **2006**, *65*, 261–268. [[CrossRef](#)]
35. Serrano, K.; Michaud, P.A.; Comninellis, C.; Savall, A. Electrochemical Preparation of Peroxodisulfuric Acid Using Boron Doped Diamond Thin Film Electrodes. *Electrochim. Acta* **2002**, *48*, 431–436. [[CrossRef](#)]
36. Lan, Y.D.; Coetsier, C.; Causserand, C.; Serrano, K.G. On the Role of Salts for the Treatment of Wastewaters Containing Pharmaceuticals by Electrochemical Oxidation Using a Boron Doped Diamond Anode. *Electrochim. Acta* **2017**, *231*, 309–318. [[CrossRef](#)]
37. Kolthoff, I.M.; Miller, I.K. The Chemistry of Persulfate.1. The Kinetics and Mechanism of the Decomposition of the Persulfate ion in Aqueous Medium. *J. Am. Chem. Soc.* **1951**, *73*, 3055–3059. [[CrossRef](#)]
38. Neta, P.; Madhavan, V.; Zemel, H.; Fessenden, R.W. Rate Constants and Mechanism of Reaction of Sulfate Radical Anion with Aromatic Compounds. *J. Am. Chem. Soc.* **1977**, *99*, 163–164. [[CrossRef](#)]
39. Yang, L.; He, L.Y.; Xue, J.M.; Ma, Y.F.; Xie, Z.Y.; Wu, L.; Huang, M.; Zhang, Z.L. Persulfate-Based Degradation of Perfluorooctanoic Acid (PFOA) and Perfluorooctane Sulfonate (PFOS) in Aqueous Solution: Review on Influences, Mechanisms and Prospective. *J. Hazard. Mater.* **2020**, *393*, 11. [[CrossRef](#)]
40. Qian, Y.J.; Guo, X.; Zhang, Y.L.; Peng, Y.; Sun, P.Z.; Huang, C.H.; Niu, J.F.; Zhou, X.F.; Crittenden, J.C. Perfluorooctanoic Acid Degradation Using UV-Persulfate Process: Modeling of the Degradation and Chlorate Formation. *Environ. Sci. Technol.* **2016**, *50*, 772–781. [[CrossRef](#)]
41. Silveira, J.E.; Garcia-Costa, A.L.; Cardoso, T.O.; Zazo, J.A.; Casas, J.A. Indirect Decolorization of Azo Dye Disperse Blue 3 by Electro-Activated Persulfate. *Electrochim. Acta* **2017**, *258*, 927–932. [[CrossRef](#)]
42. Lan, Y.; Coetsier, C.; Causserand, C.; Serrano, K.G. An Experimental and Modelling Study of the Electrochemical Oxidation Of Pharmaceuticals Using a Boron-Doped Diamond Anode. *Chem. Eng. J.* **2018**, *333*, 486–494. [[CrossRef](#)]



© 2020 by the authors. Licensee MDPI, Basel, Switzerland. This article is an open access article distributed under the terms and conditions of the Creative Commons Attribution (CC BY) license (<http://creativecommons.org/licenses/by/4.0/>).